Desalination and Water Treatment
www.deswater.com

doi: 10.5004/dwt.2020.26018

198 (2020) 232–240
September

Evaluation of adsorption performance of phenol using non-calcined Mobil composition of matter no. 41 particles

Khairi R. Kalash[a,*], Mustafa H. Al-Furaiji[a], Basma I. Waisi[b], Raad A. Ali[a]

[a]*Environment and Water Directorate, Ministry of Science and Technology, Baghdad, Iraq, Tel. 009657724042551; emails: khairirs@gmail.com (K.R. Kalash), alfuraiji79@gmail.com (M.H. Al-Furaiji), rakoka2005@yahoo.com (R.A. Ali)*
[b]*Department of Chemical Engineering, College of Engineering, University of Baghdad, Baghdad, Iraq, email: basmawaisi@coeng.uobaghdad.edu.iq (B.I. Waisi)*

Received 25 December 2019; Accepted 22 April 2020

ABSTRACT

In this research, the adsorption performance of Mobil composition of matter No. 41 (MCM-41) silica-based particles in phenol removal using batch mode operation has been studied. The effect of operating conditions like pH, adsorbent dose, mixing rate and temperature on adsorbent performance was studied. The optimum operating conditions were found to be pH = (4–9), adsorbent dose = 0.4 g, mixing rate = 200 rpm and temperature = 298 K. Phenol removal percentage at the optimal conditions was 67%. Adsorption isotherm studies showed that the Langmuir model was better in describing phenol removal using MCM-41 adsorbent indicating that monolayer adsorption is the dominant mechanism. Kinetics studies were conducted using pseudo-first-order and pseudo-second-order kinetic models. Our results showed that the pseudo-second-order model was better in representing the adsorption of phenol using MCM-41 particles.

Keywords: Adsorption; Phenol removal; MCM-41 particles; Adsorption isotherm; Wastewater treatment; Adsorption kinetics

1. Introduction

Potable water resources become more vulnerable due to the increase in world population and industrial activities [1]. Phenol is one of the major pollutants that can exist in the industrial wastewater due to the fact that it is a basic raw material in many industrial activities; it can be detected in the effluent from coking operation, petroleum refining, petrochemicals, resin manufacturing, pulp and paper mills, pharmaceuticals, and plastics [2]. Phenol has been classified as a toxic material and strict discharge limits have been set to ensure a sustainable environment. Exposure to phenol even with low limits would cause serious health hazards like diarrhea, vertigo, anorexia, weight loss, salivation, and dark coloration of the urine [3].

Removal of phenolic compounds from wastewater can be achieved using various methods including membranes, bio-degradation, advanced oxidation, and adsorption. Various membrane processes can be used to remove phenolic compounds from aqueous solutions. Khazaali et al. [4] studied the performance of reverse osmosis process in removing bisphenol and found that a maximum rejection of 87.34% can be achieved. Forward osmosis process has been used for phenol removal and rejections of about 76% and 98.8% were reported by Cui et al. [5] and Huang et al. [6] respectively. Membrane bioreactor, which combines conventional activated sludge treatment with membrane process, showed complete biodegradation of phenol [7]. Ultrafiltration coupled with nanofiltration or reverse osmosis has been

* Corresponding author.

investigated for phenol removal from paper mill wastewater. Maximum rejection of about 95% was achieved with these hybrid processes [8].

A part from membrane processes, phenol can also be biodegraded in the presence of suitable organisms under both aerobic and anaerobic conditions. The moving bed bioreactor process achieved more than 90% phenol biodegradation and can be increased to more than 99% in pH shock conditions [9]. Moussavi et al. [10] studied using a moving-bed sequencing batch reactor for the biological removal of phenol from wastewaters. This reactor had the ability to remove 99 % of the phenol from a feed containing 2,000 ppm phenol concentration.

Advanced oxidation processes which are technologies that convert complex pollutants to non-harmful inert materials also have been used in phenol removal [11]. Seid-Mohammadi et al. [12] used UV rays in an advanced oxidation process to remove high concentrations of phenol from saline wastewater. Persulfate was used as the oxidant reagent and maximum removal of 93% was reached. Also, the Fenton process has been studied in phenol removal. It was found that the Fenton process is more efficient in phenol removal at a high concentration of NaCl [13].

Adsorption has been investigated in phenol removal using various adsorbent materials.

Activated carbon which is the most widely used adsorbents especially in phenol removal can be prepared from different sources like tobacco residues [14], date stones [15], rubber seed coat [16], coconut shell [17,18], pistachio-nut shell [19], palm kernel [20] and avocado kernel seeds [21].

Recently, the use of highly porous nanoparticles as an adsorbent for phenol removal has gained more attention. Bhadra et al. [22] have employed a metal-organic framework as an adsorbent for phenol removal from fuel. Saleh et al. [23] prepared and modified silica nanoparticles for phenol removal from aqueous solutions. The maximum removal of 85% was achieved with these nanoparticles at an initial concentration of 10 mg/L of phenol. Mobil composition of matter No. 41 (MCM-41) nanoparticles have been considered as an adsorbent in removing various pollutants (organic and inorganic) from wastewater [24,25].

In this work, for the first time, the performance of the non-calcined MCM-41 particles in removing phenol from aqueous solutions was studied. Different operating conditions (i.e. pH, adsorbent dose, mixing rate, and temperature) have been studied besides the adsorption isotherms and the reaction kinetics.

2. Materials and methods

2.1. Chemicals

Phenol (≥99.5%) was purchased from Sigma-Aldrich (Germany). Cetyltrimethylammonium bromide (CTAB) [$(C_{16}H_{33})$ N $(CH_3)_3$] Br and tetraethoxysilane (TEOS) $(C_2H_5)_4$ SiO_4 were obtained from Sigma-Aldrich (Germany) (both with the purity of 98%) and were used as materials for preparing the MCM-41 particles. Sulfuric acid (H_2SO_4, purity 96%) was ordered from Biosolve (USA) while sodium hydroxide (NaOH, purity 95%) was provided by BDH (England).

2.2. Preparation of MCM-41 particles

Non-calcined MCM-41 was synthesized by adding 5.78 g of TEOS to a solution containing 0.34 g of NaOH and 1.01 g of CTAB in 30 mL of deionized water and was agitated for 60 min by a magnetic stirrer at room temperature. The obtained mixture was crystallized at a temperature of 110°C using an autoclave for 96 h. The molar composition of the gel mixture was 1.0:0.1:0.3:60 for TEOS:CTAB:NaOH:H_2O, respectively. The solid mixture was recovered by filtration, washing several times to remove the organic template and then was dried at 35°C for 24 h in order to get the non-calcined MCM-41.

2.3. Characterization of MCM-41 particles

The hexagonal structure and mesoporosity of MCM-41 were examined by X-ray diffraction (XRD) analysis using a Shimadzu-6000, (origin: Japan) at low angle X-ray diffractometer with 2θ range from 0° to 5° with scan rate 2 (°/min) and Cu-kα (λ = 1.541) as radiation source was applied. The morphology analysis of MCM-41 samples was determined using VEGA 3 LM scanning electron microscopy (SEM). The specific surface area of MCM-41 was measured using Q-surf 9600 surface area analyzer, (USA). The Fourier-transform infrared spectroscopy (FTIR) test was conducted using Bruker–Tensor 27 apparatus, (Germany). A thermogravimetric analysis (TGA) was done for thermal stability measurement. The powder was heated till 600°C, at a heating rate of 10°C/min using an STA PT1000 thermogravimetric analyzer.

2.4. Batch adsorption experiments

The standard solution was prepared by dissolving 1,000 mg of phenol in 1,000 mL deionized water to get an aqueous solution of phenol with a concentration of 1,000 mg L^{-1}. This solution was then shacked for 30 min to ensure a homogeneous distribution of the phenol. The non-MCM-41 adsorption experimentations were done after dilution of this stock solution to the desired concentration.

The effect of contact time, adsorbent dose, pH, effect of mixing speed, initial concentration of phenol and temperature on the adsorption isotherms and kinetics was studied in a batch experiment. Conical flask containing 50 mL of phenol solution and 0.4 g of non-calcined MCM-41, kept under agitation speed of 200 rpm was used for the batch experiment. The samples then centrifuged at 3,500 rpm for 3 min.

Final phenol concentrations in the residual solution were measured by UV spectrophotometer type: UV-1100 at wavelengths of 270 nm. All experimental was performed at a temperature of 25.0°C ± 0.1°C (except the experiments of temperature effect). The percentage removal of phenol and adsorption capacity (q_e) was calculated according to the following equations:

$$R\% = \frac{C_0 - C_f}{C_0} \times 100\% \quad (1)$$

$$q_e = \frac{V\left(C_0 - C_f\right)}{m} \quad (2)$$

where C_0 = initial phenol concentrations (mg/L); C_f = final phenol concentrations (mg/L); V = volume of the phenol solution (L); m = mass of the adsorbent (g).

3. Results and discussion

3.1. Characterization of non-calcined MCM-41

XRD pattern of the prepared non-calcined MCM-41 is shown in Fig. 1. It can be seen that at lower 2θ (equal to 2°) an acute peak of 100 is clearly observed. However, at higher 2θ, the other two peaks with lower intensities are measured. These three peaks confirm the formation of the hexagonal structure of the particles indicating that the prepared particles were MCM-41 [25].

Table 1 shows the physicochemical properties of calcined MCM-41 and non-calcined MCM-41 from our previous study. The pore volume and Brunauer–Emmett–Teller (BET) surface area of non-calcined MCM-41 were found to be 0.101 cm^3/g and 28.7 m^2/g, respectively, which are less than that of calcined MCM-41 (1,000 m^2/g and 0.978 cm^3/g, respectively).

The surface morphology and particle distribution of the prepared silica MCM-41 grains are clarified in Fig. 2. The sample has irregular aggregates with a wide particle size distribution with some cavities and pores of different sizes and different shapes. The energy dispersive analysis of X-rays (EDAX) spectrum of MCM-41 is shown in Fig. 3. EDAX analysis showed the chemical composition of MCM-41 is 54.9% oxygen and 45.1% silica.

FTIR depicted in Fig. 4 shows the strong broad peak near 3,470 cm^{-1} due to surface hydroxyl group (OH) and adsorbed water molecules asymmetric stretching vibration absorption [26]. The peak at 1,630 cm^{-1} designates the stretching vibration of H–OH. The intensity appeared near 2,900 cm^{-1} corresponds to the stretching vibration of the CH bond. The absorption peak at 1,090 and 960 cm^{-1} corresponds to the Si–O–Si bond and Si–O in silanol groups, respectively symmetric stretching vibration of the MCM-41 skeleton [27]. At absorption peak at 1,490 cm^{-1} correspond to the bending vibration of ammonium ions. The three peaks at 2,900; 2,860 and 1,490 cm^{-1} create from the organic surfactant template present in non-calcined MCM-41, which cannot be found in calcined MCM-41. The peaks at 480 and 800 cm^{-1} are attributed to Si–O stretching vibration and bending vibration of Si–O tetrahedron [28].

TGA was used to study the thermal stability of MCM-41 material by monitoring the weight change that occurs as a sample is heated up from 30°C to 600°C at a constant rate. As shown in Fig. 5, the weight losses 9.55% showing consecutively decreasing trend as temperature rises from 30°C to 158°C, which was mainly due to the removal of adsorbed water. Moreover, the uncondensed hydroxyl groups cover the pores and make them polar channel. From 158°C to about 267°C, the loss of 5.2% for MCM-41 was might be attributed to the decomposition of surfactant. At temperatures from 267°C–600°C, the weight loss was most likely to the decomposition of the organosilane groups [29].

3.2. Batch adsorption experiments

The impact of changing the operating conditions on phenol removal efficiency using silica MCM-41 was investigated

Table 1
Characterizations of calcined MCM-41 and non-calcined MCM-41 particles [25]

Material	Calcined MCM-41	Non-calcined MCM-41
S_{BET} (m^2/g)	1,000	28.7
V (cm^3/g)	0.978	0.101
D_{BJH} (nm)	3.406	2.513
d_{100} (nm) XRD	4.41	4.72
a_0 (nm) XRD	5.09	5.45
Si wt.% EDAX	43.5	45.1
O_2 wt.% EDAX	56.5	54.9

S_{BET}: BET surface area; V: volume of pore; D_{BJH}: diameter of pore; d_{100}: $d_{(100)}$ spacing; a_0: center–center distance ($a_0 = (2/\sqrt{3})\ d$.

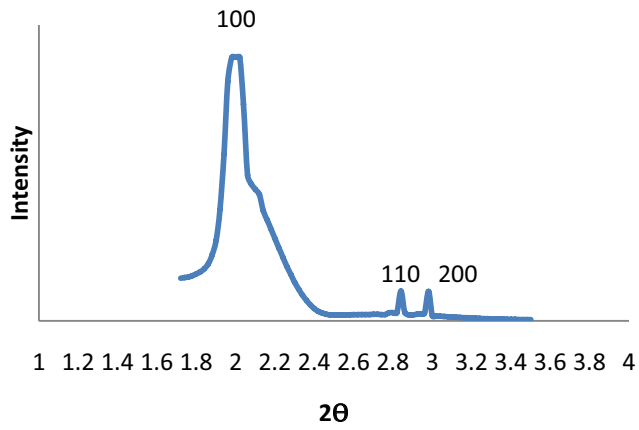

Fig. 1. XRD pattern of the non-calcined MCM-41 particles.

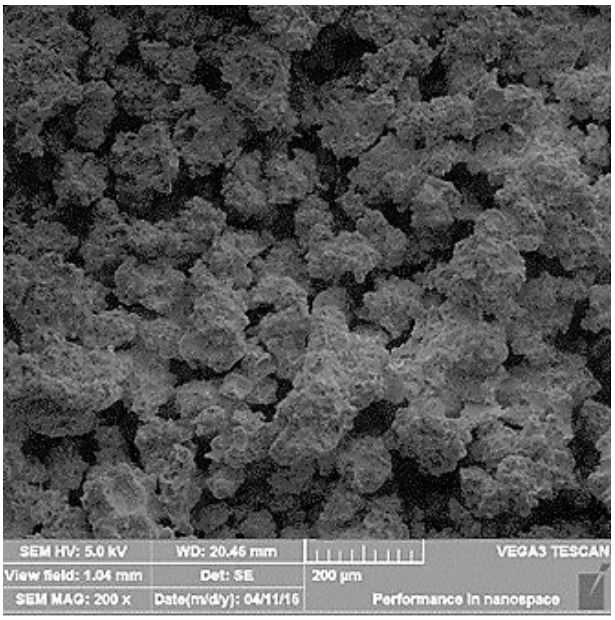

Fig. 2. SEM image of the non-calcined MCM-41 particles.

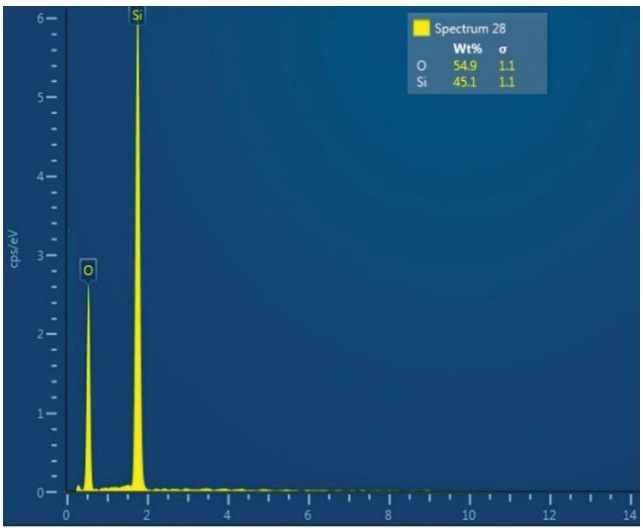

Fig. 3. EDAX of the non-calcined MCM-41 particles.

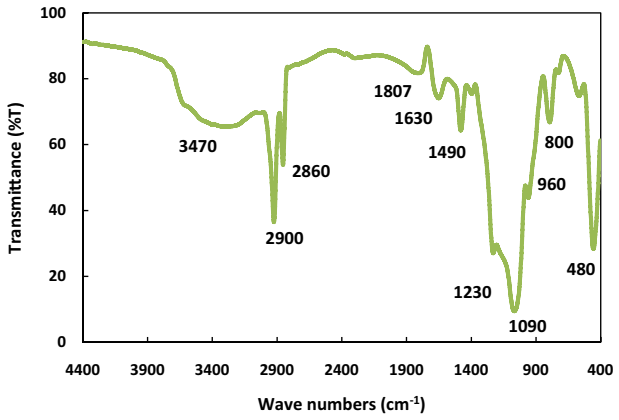

Fig. 4. FTIR spectra of non-calcined MCM-41 particles.

at different ranges. Each experiment was duplicated, and a good reproducibility was observed. Here the impact of varying each parameter at the optimum values of the other parameters will be presented.

3.2.1. Effect of pH

The pH of the aqueous solutions has a high effect on the surface charge of the adsorbent and the ionization degree of the adsorbate [21,30]. As a result, the pH effect needs to be evaluated the adsorption experiments were conducted with initial phenol concentration of 25 mg L^{-1} and MCM-41 concentration of 0.4 g L^{-1} by changing the pH of the solutions over a range of 2–11 (Fig. 6). An obvious increase occurred when pH increased from 2 to 4 reaching a removal efficiency of 65%. At further increase in pH, Phenol removal percentage showed an almost constant level till pH value 9. However, beyond this value of pH, the adsorption of phenol decreases sharply. Increasing the affinity of phenol to non-calcined MCM-41 surface at acidic medium can be explained by the negative charge of the hydroxyl group in phenol. Phenol as a weak acid compound with (acidity constant) pKa value of 9.9 is dissociated at pH > pKa [31]. As a result, at higher pH values, the ionization degree of phenol and presence of additional hydroxyl ions thus the diffusion of phenolic ions are hindered, and the electrostatic repulsion between phenol and the negatively charged surface sites of the adsorbent at ions increases. A similar result was observed for the adsorption of phenol by organo modified tirebolu bentonite [32].

3.2.2. Effect of adsorbent dose

The amount of surface available for the adsorption process is an important parameter because adsorption is mainly a surface phenomenon. Consequently, the adsorbent dose has a considerable effect on the adsorption efficiency. The adsorbent dosage determines the capacity of adsorbent for a specific phenol concentration and also determines the

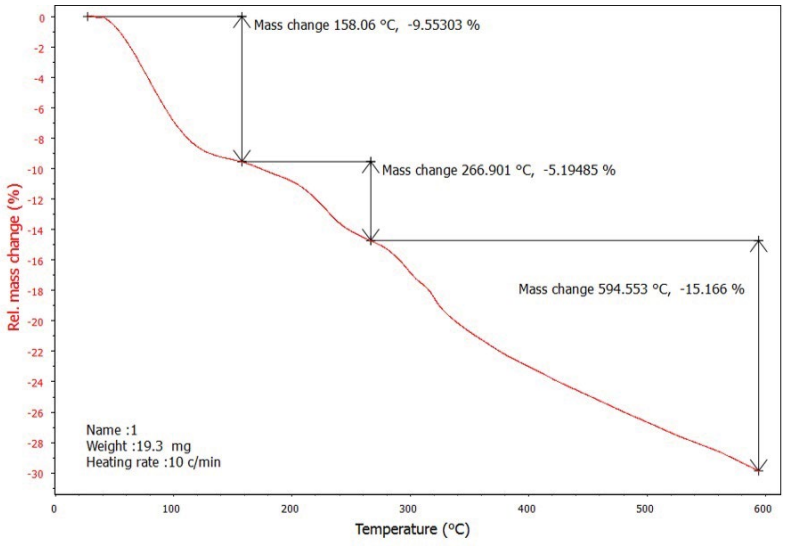

Fig. 5. TGA analysis of the non-calcined MCM-41 particles.

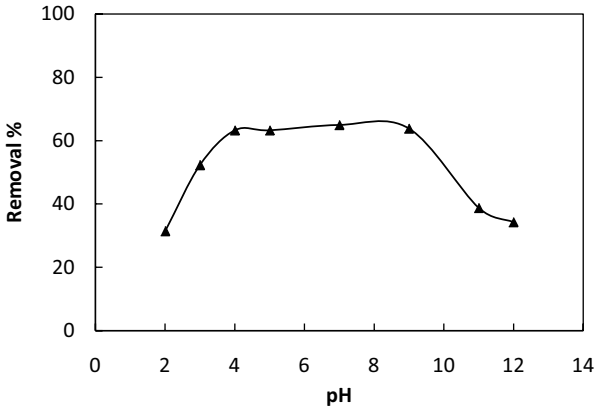

Fig. 6. pH effect on removal of phenol.

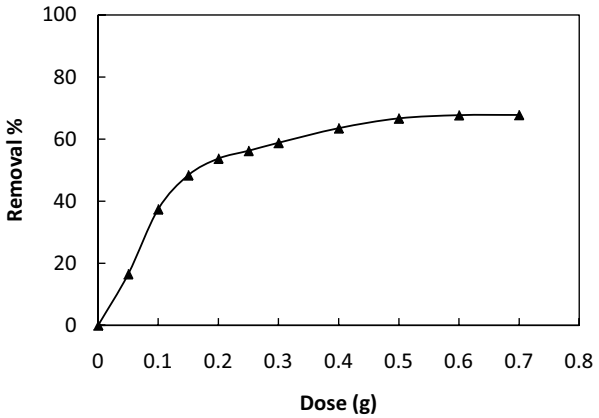

Fig. 7. Effect of MCM-41 dose on the removal of phenol.

equilibrium conditions between the sorbent and sorbate of the system. The effect of MCM-41 dosage on the adsorption of phenol was investigated using different amounts of MCM-41 in the range of 0.05–0.7 g/L. the initial phenol concentration was 25 mg L^{-1} at pH 7.0. Fig. 7 phenol shows phenol removal efficiency as a function adsorbent dose. Phenol removal clearly increased from 16.5% to 63% with increasing MCM-41 dose from 0.05 to 0.4 g due to the greater surface area and a number of active sites for binding phenol molecules on the adsorbent and thus more phenol was attached to their surface. However, after the adsorbent dose of 0.4 g/L, the removal efficiency did not change with further increase in adsorbent dosage [32]. As a result, silica MCM-41 dose for further adsorption experiments 0.4 g/L was selected as the adsorbent optimum amount, and the relevant q_e reached 2.22 mg/g. The uptake of non-calcined MCM-41 for phenol is larger than that of some adsorbents, such as zeolitic composite (0.5325 mg/g) [33] and activated carbon (1.1989 mg/g) [34]. In addition, non-calcined MCM-41 can completely be mixed and easily separated from the aqueous solution. As a result, non-calcined MCM-41 can be considered as an effective absorbent for wastewater treatment.

3.2.3. Effect of mixing rate

Fig. 8 represents the effect of the stirring speed (100–200 rpm) on phenol removal percentage. The maximum phenol ions removal increased up to 200 rpm because stirring provides proper interactions between phenol molecules in solution and the adsorbent binding sites and reduces the mass transfer boundary layer thickness allowing phenol to reach the surface of the sorbent. This data approves that external mass transport resistance has a noticeable effect on the kinetics of the adsorption process. Therefore 200 rpm was selected for subsequent study.

3.2.4. Effect of temperature

Temperature is an important factor to know the adsorption nature whether it is an exothermic or endothermic process. Increasing the pollutant removal percentage with increasing temperature means that the adsorption is an endothermic process that might occur due to increasing the mobility of the phenol toward the adsorption active

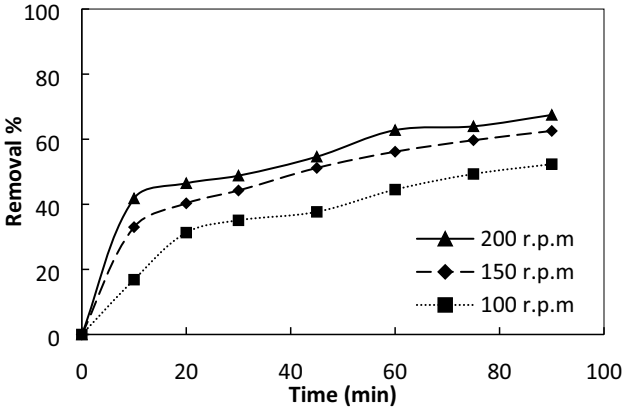

Fig. 8. Effect of mixing speed on the removal of phenol.

sites [35]. In other cases, the rising temperature may reduce the adsorptive forces between the active sites on the adsorbent surface and the pollutant molecules leading to reducing adsorption efficiency indicating that the process is exothermic [36].

To evaluate the temperature effect, the uptake of phenol onto silica MCM-41 was tested by increasing the temperature from 25°C–45°C at optimum conditions as shown in Fig. 9. The maximum removal was observed at 25°C, further increase in temperature leads to the decrease in removal percent which can be considered as an indicator that the phenol uptake onto MCM-41 grains mostly followed the exothermic nature of the adsorption process. These results can be explained by the weakening of the sorption forces with increasing the temperature. It is also can be assigned to the role of the temperatures in enhancing the solubility of phenol in the solution resulting in increasing the attraction forces between phenol and the solution which minimizes its uptake on MCM-41 grains surface. This is compatible with the previous result, which showed a decrease in the removal percentage with further increasing temperature [32,36].

3.3. Analysis according to isotherms

Adsorption isotherm study is of importance in identifying the equilibrium behavior of adsorption and describing

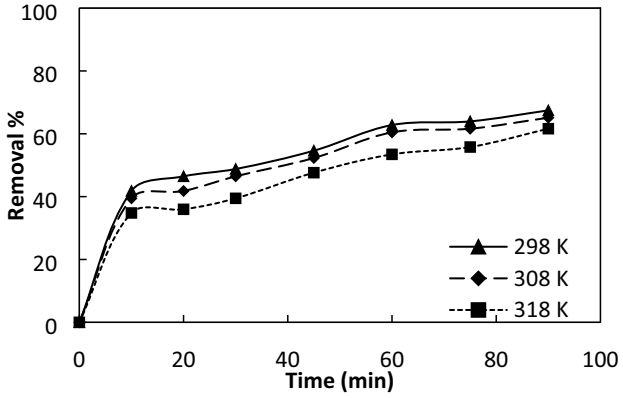

Fig. 9. Effect of temperature on the removal of phenol.

the interaction between the adsorbates and adsorbents under the optimum conditions. The most commonly used isotherm models are well-known Langmuir, Freundlich and Temkin. The Langmuir adsorption isotherm explains adsorption by assuming the adsorbent surface is homogeneous and has a finite and monolayer capacity to adsorb the sorbate. Once a molecule occupies a site, no further adsorption takes place at that site. Therefore, the Langmuir isotherm model was chosen for the estimation of the maximum adsorption capacity. Langmuir model can be represented by the expression:

$$q = \frac{q_{\max} \cdot K_L \cdot C_e}{1 + K_L \cdot C_e} \tag{3}$$

where $q_{\max}$ is the maximum amount of removed phenol per unit weight of MCM-41 (mg/g), C_e is the concentration at equilibrium (mg/L), and K_L is the constant related to the free energy of adsorption (L/mg) [37]. The low values of K_L indicate a high affinity of MCM-41 to phenol. The linear form of Eq. (3) is represented as Eq. (4):

$$\frac{C_e}{q} = \frac{1}{q_{\max} \cdot K_L} + \frac{C_e}{q_{\max}} \tag{4}$$

where $q_{\max}$ and K_L can be determined from the slope and intercept of the linear plot of C_e/q vs. C_e.

The Freundlich isothermal model describes a heterogeneous multi-layer adsorption systems. This model assumes that increasing the adsorbate concentration leads to increasing the concentration of adsorbate on the adsorbent surface. The Freundlich isotherm is expressed as Eq. (5):

$$q = K_f \cdot C_e^{\left(\frac{1}{n}\right)} \tag{5}$$

where K_F and n are Freundlich's adsorption capacity and adsorption strength constants of the adsorbent, respectively. Both K_F and $1/n$ can be obtained from the intercept and slope of the linear plot of $\ln q_e$ vs. $\ln C_e$. The higher the values of these constants indicates the higher the affinity of adsorbent to adsorbate [38].

The other isothermal model is Temkin isotherm which explicitly takes into account the adsorbent–adsorbate interactions. This model is based on assuming the adsorption heat of the whole number of molecules in the layer reduces linearly with coverage owing to adsorbent–adsorbate interactions. Also, this model assumes that the adsorption is described by a consistent spread of binding energies, reaching almost peak binding energy [39]. Temkin isothermal model can be stated by Eq. (6):

$$q_e = \frac{RT}{b_T} \ln K_T C_e \tag{6}$$

where q_e is the amount of adsorbed phenol per adsorbent unit weight (mg/g), K_T is the constant of equilibrium binding (L/g) relevant to the peak binding energy, B is the constant of Temkin isotherm and is connected to the heat adsorption

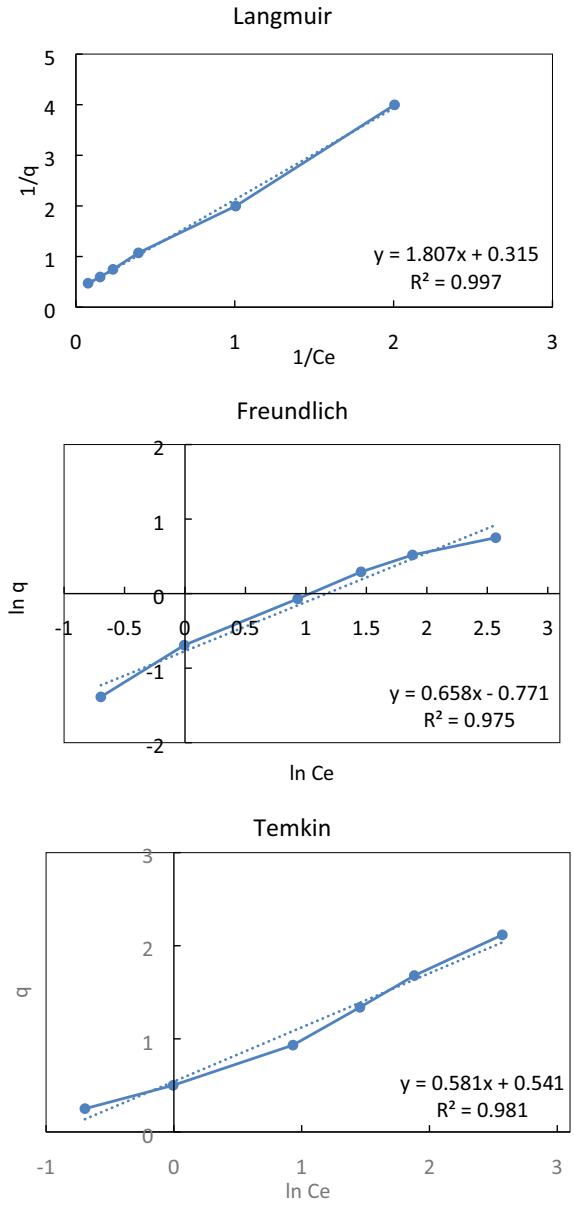

Fig. 10. (a) Langmuir, (b) Freundlich, and (c) Temkin models for adsorption of phenol on MCM-41 particles.

heat (kJ/mol), and C_e is the concentration of adsorbate in solution at equilibrium (mg/L). Eq. (5) can be written in the linear form as follows:

$$q_e = B\ln K_T + B\ln C_e \tag{7}$$

where, $B = R_T/b_T$.

Fig. 10 shows the obtained data of Langmuir, Freundlich and Temkin adsorption isotherms of phenol by MCM-41. Table 2 summarizes the constants coefficients (K_L, q_{max}, K_F, n, K_T, and B) of Langmuir, Freundlich and Temkin models obtained in this study for phenol uptake. Identifying the best model that describes phenol adsorption is done based on the higher correlation coefficient (R^2) obtained from each model. However, the applicability of all three models which can be noticed from the close values of $R^2 > 0.95$ indicates that both kinetics (i.e. monolayer adsorption and heterogeneous surface situations) occur under the experimental conditions of this investigation. The value of $n = 1.52$ indicated that the adsorption was easy and confirmed that silica MCM-41 materials were possible to obtain high adsorption. Also, the positive value of B indicated that the phenol uptake onto MCM-41 is exothermic adsorption process.

3.4. Adsorption kinetics

The adsorption kinetics is essential to understand the mechanism of the adsorption indicating the adsorption rate [40]. The common kinetic models are the pseudo-first-order and the pseudo-second-order.

The pseudo-first-order equation can be written as follows [40]:

$$\ln\left(q_e - q_t\right) = \ln q_e - k_1 t \tag{8}$$

where q_e and q_t are the amounts of phenol adsorbed (mg/g) at equilibrium and at time t, respectively, k_1 (1/min) is the pseudo-first-order rate constant. The values of q_e and k_1 can be determined from the intercept and slope of the plot $\ln(q_e - q_t)$ vs. t, respectively.

The other kinetic model is the pseudo-second-order model which is represented in the following form [41]:

$$\frac{t}{q_t} = \frac{1}{k_1 \cdot q_e^2} + \frac{t}{q_t} \tag{9}$$

where k_2 (g/mg min) is the rate constant of the second-order equation. The plot of t/q_t vs. t should give a straight line (Fig. 11) if the pseudo-second-order kinetic model is applicable and q_e and k_2 can be determined from slope and intercept of the plot, respectively.

Table 3 presents the values of q_e, k_2 along with the correlation coefficients for the pseudo-first-order and pseudo-second-order models. The value of the correlation coefficient for the pseudo-second-order kinetic model is very high

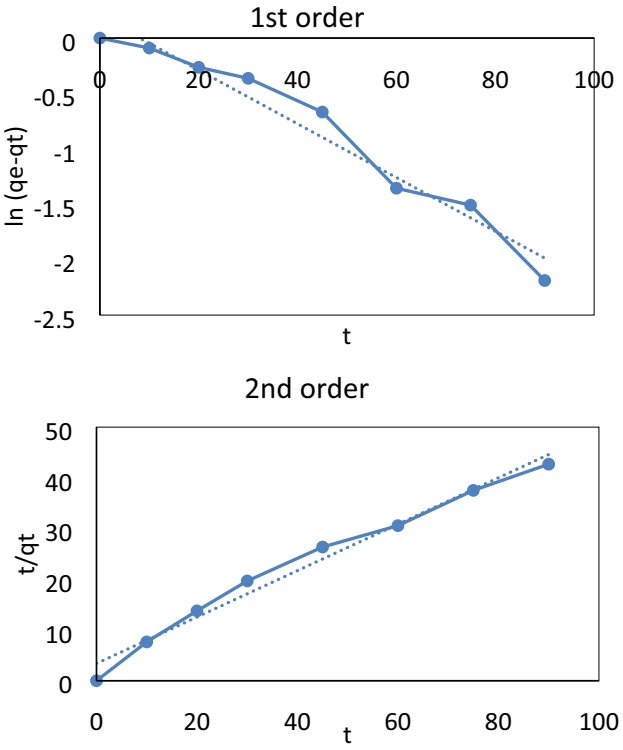

Fig. 11. Adsorption kinetics of MCM-41 particles toward phenol.

Table 2
Langmuir, Freundlich and Temkin coefficients for adsorption of phenol on MCM-41

Adsorbent	Langmuir			Freundlich			Temkin		
	q_{max} (mg/g)	K_L (L/mg)	R_L^2	K_F (mg/g)	n	R_F^2	K_T (L/mg)	B	R_T^2
MCM-41	3.172	0.174	0.997	0.463	1.519	0.975	0.394	0.581	0.981

Table 3
Pseudo-first-order and pseudo-second-order rate constants of phenol adsorption

Adsorbent	$q_{e,exp}$ (mg/g)	Pseudo-first-order			Pseudo-second-order		
		$q_{e,cal}$ (mg/g)	k_1 (min^{-1})	R^2	$q_{e,cal}$ (mg/g)	k_2 (g/mg min)	R^2
MCM-41	2.222	1.215	0.024	0.958	2.185	0.062	0.981

(R^2 = 0.98) and the calculated $q_{e,\text{cal}}$ value is very close to the experimental $q_{e,\text{exp}}$ value. As a result, phenol adsorption by MCM-41 can be well represented by the pseudo-second-order model in contrast to the pseudo-first-order model.

4. Conclusion

The results of this work indicate that non-calcined MCM-41 was successfully prepared with a microporous and hexagonal structure. Also, the results show that MCM-41 is an effective adsorbent for phenol removal from contaminated water with a removal percentage of 67% using 0.4 g of MCM-41, mixing rate of 200 rpm, pH value between 4 and 9, and at room temperature. The adsorption mechanism was found to be mainly surface adsorption isotherm which is represented by Langmuir isotherm. It showed a better fit than the Freundlich isotherm, thus, indicating the applicability of monolayer coverage of phenol on MCM-41 surface. The pseudo-second-order kinetic model accurately described the adsorption kinetics. Increasing the temperature decreased the phenol removal rate but the maximum adsorption capacity was similar. It is highly recommended to study the performance of the functionalized MCM-41 particles in the adsorption of phenols.

References

[1] K.R. Kalash, M.A. Kadhom, M.H. Al-Furaiji, Short-cut nitrification of Iraqi municipal wastewater for nitrogen removal in a single reactor, IOP Conf. Ser.: Mater. Sci. Eng., 518 (2019) 022024.

[2] S. Mohammadi, A. Kargari, H. Sanaeepur, K. Abbassian, A. Najafi, E. Mofarrah, Phenol removal from industrial wastewaters: a short review, Desal. Water Treat., 53 (2015) 2215–2234.

[3] L.G.C. Villegas, N. Mashhadi, M. Chen, D. Mukherjee, K.E. Taylor, N. Biswas, A short review of techniques for phenol removal from wastewater, Curr. Pollut. Rep., 2 (2016) 157–167.

[4] F. Khazaali, A. Kargari, M. Rokhsaran, Application of low-pressure reverse osmosis for effective recovery of bisphenol A from aqueous wastes, Desal. Water Treat., 52 (2014) 7543–7551.

[5] Y. Cui, X.-Y. Liu, T.-S. Chung, M. Weber, C. Staudt, C. Maletzko, Removal of organic micro-pollutants (phenol, aniline and nitrobenzene) via forward osmosis (FO) process: evaluation of FO as an alternative method to reverse osmosis (RO), Water Res., 91 (2016) 104–114.

[6] Y.B. Huang, P. Cay-Durgun, T.M. Lai, P. Yu, M.L. Lind, Phenol removal from water by polyamide and AgCl mineralized thin-film composite forward osmosis membranes, Ind. Eng. Chem. Res., 57 (2018) 7021–7029.

[7] B. Marrot, A. Barrios-Martinez, P. Moulin, N. Roche, Biodegradation of high phenol concentration by activated sludge in an immersed membrane bioreactor, Biochem. Eng. J., 30 (2006) 174–183.

[8] X.F. Sun, C. Wang, Y.B. Li, W.G. Wang, J. Wei, Treatment of phenolic wastewater by combined UF and NF/RO processes, Desalination, 355 (2015) 68–74.

[9] H. Zhou, G.C. Wang, M.H. Wu, W.P. Xu, X.W. Zhang, L.F. Liu, Phenol removal performance and microbial community shift during pH shock in a moving bed biofilm reactor (MBBR), J. Hazard. Mater., 351 (2018) 71–79.

[10] G. Moussavi, M. Mahmoudi, B. Barikbin, Biological removal of phenol from strong wastewaters using a novel MSBR, Water Res., 43 (2009) 1295–1302.

[11] Y.D. Shahamat, M. Farzadkia, S. Nasseri, A.H. Mahvi, M. Gholami, A. Esrafili, Magnetic heterogeneous catalytic ozonation: a new removal method for phenol in industrial wastewater, J. Environ. Health Sci. Eng., 12 (2014) 50.

[12] A. Seid-Mohammadi, G. Asgari, A. Poormohammadi, M. Ahmadian, H. Rezaeivahidian, Removal of phenol at high concentrations using UV/Persulfate from saline wastewater, Desal. Water Treat., 57 (2016) 19988–19995.

[13] R. Maciel, G.L. Sant'Anna Jr., M. Dezotti, Phenol removal from high salinity effluents using Fenton's reagent and photo-Fenton reactions, Chemosphere, 57 (2004) 711–719.

[14] M. Kilic, E. Apaydin-Varol, A.E. Pütün, Adsorptive removal of phenol from aqueous solutions on activated carbon prepared from tobacco residues: equilibrium, kinetics and thermodynamics, J. Hazard. Mater., 189 (2011) 397–403.

[15] S.K. Dhidan, Removal of phenolic compunds from aqueous solutions by adsoption onto activted carbons prepared from date stones by chemical activation with $FeCl_3$, J. Eng., 18 (2012) 63–77.

[16] S. Rengaraj, S.-H. Moon, R. Sivabalan, B. Arabindoo, V. Murugesan, Removal of phenol from aqueous solution and resin manufacturing industry wastewater using an agricultural waste: rubber seed coat, J. Hazard. Mater., 89 (2002) 185–196.

[17] R.R. Karri, J.N. Sahu, N.S. Jayakumar, Optimal isotherm parameters for phenol adsorption from aqueous solutions onto coconut shell based activated carbon: error analysis of linear and non-linear methods, J. Taiwan Inst. Chem. Eng., 80 (2017) 472–487.

[18] R.R. Karri, N.S. Jayakumar, J.N. Sahu, Modelling of fluidised-bed reactor by differential evolution optimization for phenol removal using coconut shells based activated carbon, J. Mol. Liq., 231 (2017) 249–262.

[19] E. Bazrafshan, F.K. Mostafapour, A.H. Mahvi, Phenol removal from aqueous solutions using pistachio-nut shell ash as a low cost adsorbent, Fresenius Environ. Bull., 21 (2012) 2962–2968.

[20] M.N. Hairuddin, N.M. Mubarak, M. Khalid, E.C. Abdullah, R. Walvekar, R.R. Karri, Magnetic palm kernel biochar potential route for phenol removal from wastewater, Environ. Sci. Pollut. Res., 26 (2019) 35183–35197.

[21] L.A. Rodriguesa, M.L.C.P. da Silva, M.O. Alvarez-Mendes, A. dos Reis Coutinho, G.P. Thim, Phenol removal from aqueous solution by activated carbon produced from avocado kernel seeds, Chem. Eng. J., 174 (2011) 49–57.

[22] B.N. Bhadra, I. Ahmed, S.H. Jhung, Remarkable adsorbent for phenol removal from fuel: functionalized metal–organic framework, Fuel, 174 (2016) 43–48.

[23] S. Saleh, A. Younis, R. Ali, E. Elkady, Phenol removal from aqueous solution using amino modified silica nanoparticles, Korean J. Chem. Eng., 36 (2019) 529–539.

[24] P. Pattanaik, N. Panigrahi, J. Mishra, N.K. Sahoo, B.P. Dash, D. Rath, Evaluation of MCM-41 nanoparticles for removal of phenol contents from coke-oven wastewater, J. Hazard. Toxic Radioact. Waste., 22 (2018) 04018001.

[25] T.M. Albayati, K.R. Kalash, Polycyclic aromatic hydrocarbons adsorption from wastewater using different types of prepared mesoporous materials MCM-41 in batch and fixed bed column, Process Saf. Environ. Prot., 133 (2020) 124–136.

[26] A. Bernal-ballen, J.-A. Lopez-Garcia, K. Ozaltin, (PVA/chitosan/fucoidan)-ampicillin: a bioartificial polymeric material with combined properties in cell regeneration and potential antibacterial features, Polymers (Basel), 1325 (2019) 1–14.

[27] H. Aguiar, J. Serra, P. González, B. León, Structural study of sol–gel silicate glasses by IR and Raman spectroscopies, J. Non-Cryst. Solids, 355 (2009) 475–480.

[28] Z.P. Fu, M. Li, B.F. Yang, R.C. Liu, Intense ultraviolet photoluminescence from amorphous Si:O:C films prepared by liquid–solution-phase technique, Thin Solid Films, 389 (2001) 12–15.

[29] N. Rahmat, N.F.M. Yusof, E. Hafiza, Thermogravimetric analysis (TGA) profile of modified SBA-15 at different amount of alkoxysilane group, Malaysian J. Anal. Sci., 18 (2014) 730–736.

[30] E. Bazrafshan, P. Amirian, A.H. Mahvi, A. Ansari-Moghaddam, Application of adsorption process for phenolic compounds removal from aqueous environments: a systematic review, Global Nest J., 18 (2016) 146–163.

[31] A.H. Aktaş, N. Şanlı, G. Pekcan, Spectrometric determination of pK_a values for some phenolic compounds in acetonitrile – water mixture, Acta Chim. Slov., 53 (2006) 214–218.
[32] H.B. Senturk, D. Ozdes, A. Gundogdu, C. Duran, M. Soylak, Removal of phenol from aqueous solutions by adsorption onto organomodified Tirebolu bentonite: equilibrium, kinetic and thermodynamic study, J. Hazard. Mater., 172 (2009) 353–362.
[33] O.B. Spiridon, E. Preda, A. Botez, L. Pitulice, Phenol removal from wastewater by adsorption on zeolitic composite, Environ. Sci. Pollut. Res., 20 (2013) 6367–6381.
[34] A.R. Khan, T.A. Al-Bahri, A. Al-Haddad, Adsorption of phenol based organic pollutants on activated carbon from multi-component dilute aqueous solutions, Water Res., 31 (1997) 2102–2112.
[35] S. Senthilkumaar, P. Kalaamani, C.V. Subburaam, Liquid phase adsorption of Crystal violet onto activated carbons derived from male flowers of coconut tree, J. Hazard. Mater., 136 (2006) 800–808.
[36] A.E. Ofomaja, Y.-S. Ho, Equilibrium sorption of anionic dye from aqueous solution by palm kernel fibre as sorbent, Dyes Pigm., 74 (2007) 60–66.
[37] N. Jiang, R. Shang, S.G.J. Heijman, L.C. Rietveld, Adsorption of triclosan, trichlorophenol and phenol by high-silica zeolites: adsorption efficiencies and mechanisms, Sep. Purif. Technol., 235 (2020) 1–9.
[38] L. Li, X.M. Wang, D.X. Zhang, R.B. Guo, X.Z. Du, Excellent adsorption of ultraviolet filters using silylated MCM-41 mesoporous materials as adsorbent, Appl. Surf. Sci., 328 (2015) 26–33.
[39] K.Y. Foo, B.H. Hameed, Insights into the modeling of adsorption isotherm systems, Chem. Eng. J., 156 (2010) 2–10.
[40] N. Thinakaran, P. Baskaralingam, M. Pulikesi, P. Panneerselvam, S. Sivanesan, Removal of Acid Violet 17 from aqueous solutions by adsorption onto activated carbon prepared from sunflower seed hull, J. Hazard. Mater., 151 (2008) 316–322.
[41] C.-Y. Kuo, C.-S. Wu, J.-Y. Wu, Adsorption of direct dyes from aqueous solutions by carbon nanotubes: determination of equilibrium, kinetics and thermodynamics parameters, J. Colloid Interface Sci., 327 (2008) 308–315.